# CHATCELL: Facilitating Single-Cell Analysis with Natural Language

**Yin Fang**[♡♣*], **Kangwei Liu**[♡♣*], **Ningyu Zhang**[♡♣†], **Xinle Deng**[♡♣], **Penghui Yang**[♡], **Zhuo Chen**[♡♣], **Xiangru Tang**[♠], **Mark Gerstein**[♠], **Xiaohui Fan**[♡], **Huajun Chen**[♡♣†]
[♡]Zhejiang University [♠]Yale University
[♣]Zhejiang University - Ant Group Joint Laboratory of Knowledge Graph
{fangyin,zhangningyu}@zju.edu.cn

https://zjunlp.github.io/project/ChatCell

## Abstract

As Large Language Models (LLMs) rapidly evolve, their influence in science is becoming increasingly prominent. The emerging capabilities of LLMs in task generalization and free-form dialogue can significantly advance fields like chemistry and biology. However, the field of single-cell biology, which forms the foundational building blocks of living organisms, still faces several challenges. High knowledge barriers and limited scalability in current methods restrict the full exploitation of LLMs in mastering single-cell data, impeding direct accessibility and rapid iteration. To this end, we introduce CHATCELL, which signifies a paradigm shift by facilitating single-cell analysis with natural language. Leveraging vocabulary adaptation and unified sequence generation, CHATCELL has acquired profound expertise in single-cell biology and the capability to accommodate a diverse range of analysis tasks. Extensive experiments further demonstrate CHATCELL's robust performance and potential to deepen single-cell insights, paving the way for more accessible and intuitive exploration in this pivotal field. [1]

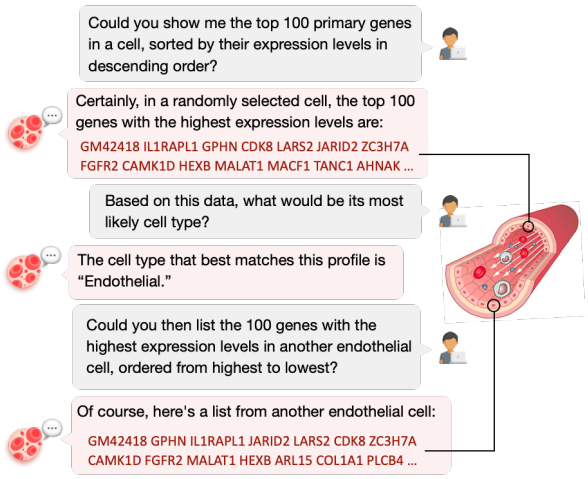


Figure 1: CHATCELL facilitates single-cell analysis through conversational interactions. Black and red texts denote human and single-cell language, respectively.

## 1 Introduction

Artificial Intelligence for Science (AI4Science) has emerged as a pivotal force in advancing scientific research (Wang et al., 2023; Tinn et al., 2023), particularly in complex domains like nuclear fusion (Degrave et al., 2022), protein structure prediction (Jumper et al., 2021), and autonomous chemical discovery (Daniil et al., 2023). Among the various AI tools, Large Language Models (LLMs) are at the forefront, demonstrating significant advancements in fields such as biology and chemistry (Zheng et al., 2023; Fang et al., 2024b; Zhang et al., 2024). These models excel in interpreting biological sequential data and following human instructions (Tong and Zhang, 2023; Fang et al., 2024a), making human language an essential medium for acquiring biological insights. As a result, LLMs are breaking down barriers to biological knowledge, revolutionizing research paradigms, and deepening our understanding of life sciences.

This paradigm shift opens new avenues for single-cell biology research, a field pivotal to understanding the basic units of life. Single-cell biology examines the intricate functions of these cells, ranging from energy production to genetic information transfer (Bechtel, 2006), playing a critical role in unraveling the fundamental principles of life and mechanisms influencing health and disease (Pollard et al., 2022). The field has witnessed a surge in single-cell RNA sequencing (scRNA-seq) data, driven by advancements in high-throughput sequencing and reduced costs. Repositories like the Gene Expression Omnibus (GEO) (Barrett et al., 2012) and the Human Cell Atlas (HCA) (Regev et al., 2017) have been instrumental in accumulating and disseminating this data. The emerging field of single-cell foundation models, such as scBERT

[*] Equal contribution.
[†] Corresponding Author.
[1] https://github.com/zjunlp/ChatCell

and scGPT (Yang et al., 2022; Theodoris et al., 2023; Cui et al., 2023; Mo et al., 2021), is changing traditional task-specific approaches (Lieberman et al., 2018; Shao et al., 2021; Liao et al., 2022). These models leverage extensive scRNA-seq datasets, applying NLP techniques to analyze gene expression matrices—structured formats that simplify scRNA-seq data into computationally tractable representations—during pre-training. They are subsequently fine-tuned for distinct single-cell analysis tasks, as shown in Figure 2(a). Despite their potential, the technical intricacies and knowledge prerequisites of these models pose challenges to their accessibility and practical application, especially in fast-paced iteration scenarios.

Recent efforts have begun to adapt LLMs for key single-cell analysis tasks, such as employing ChatGPT for cell type annotation (Hou and Ji, 2023), transforming cells into gene name sequences for cell generation (Levine et al., 2023), and developing single-cell language models for drug sensitivity analysis (Zhao et al., 2023). However, these applications demonstrate limited scalability and remain task-specific, not yet reaching the full potential of LLMs in comprehending single-cell data for more extensive single-cell analysis.

In this study, we introduce CHATCELL, a novel approach that leverages natural language to enhance single-cell analysis. Initially, we convert scRNA-seq data into a single-cell language that LLMs can readily interpret. Subsequently, we employ templates to integrate this single-cell language with task descriptions and target outcomes, creating comprehensive single-cell instructions. To improve the LLM's expertise in the single-cell domain, we conduct vocabulary adaptation, enriching the model with a specialized single-cell lexicon. Following this, we utilize unified sequence generation to empower the model to adeptly execute a range of single-cell tasks. As illustrated in Figure 1, CHATCELL allows researchers to input instructions in either natural or single-cell language, thereby facilitating the execution of necessary tasks in single-cell analysis.

The main contributions are as follows:

- We present CHATCELL, a new paradigm that leverages natural language to make single-cell analysis more accessible and intuitive.
- We enhance CHATCELL's proficiency through vocabulary adaptation, instilling it with a specialized lexicon to refine its precision in interpreting and processing single-cell data.
- We employ unified sequence generation techniques to broaden CHATCELL's capability in understanding single-cell concepts and in performing diverse tasks, thereby expanding its field applicability.
- We conduct a comprehensive evaluation of CHATCELL on essential single-cell analysis tasks, including random cell generation, pseudo-cell generation, cell type annotation, and drug sensitivity prediction. Further analysis highlights CHATCELL's potential to offer valuable biological insights.

## 2 Related Work

**Single-cell analysis.** Single-cell analysis delves into the examination and manipulation of individual cells, aiming to decipher their specific roles in complex biological systems. This discipline leverages scRNA-seq to reveal the active genes and their expression levels within single cells (Plass et al., 2018; Cao et al., 2019). For efficient analysis, scRNA-seq data is organized into gene expression matrices, where columns and rows correspond to individual cells and genes, respectively, and the matrix values reflect gene expression levels (Brazma and Vilo, 2000). Utilizing these matrices enables researchers to handle a range of critical tasks in single-cell analysis, such as dissecting the cellular composition of tissues and identifying novel cell types and states. The challenges in this field, including managing high-dimensional data (Wu and Zhang, 2020; Tejada-Lapuerta et al., 2023), addressing data sparsity (Bouland et al., 2023), and handling the computational demands of large-scale data analysis (Wolf et al., 2018), are being addressed by the development of innovative computational tools and algorithms. These advancements are crucial for distilling reliable and biologically relevant insights from single-cell data.

**Single-cell foundation models.** Initial attempts to analyze gene expression matrics involve machine learning methods and autoencoder-based approaches (Liu et al., 2021; Oller-Moreno et al., 2021; Ji et al., 2021). However, these studies often produce models tailored for specific tasks, which lack the adaptability for broader analytical applications (Angerer et al., 2017). Inspired by the

success of foundation models in NLP tasks (Devlin et al., 2019; Lewis et al., 2020), the concept is naturally extended to the single-cell domain. Single-cell foundation models emerge to offer wide-ranging capabilities across various single-cell analysis tasks. ScBERT (Yang et al., 2022) acquires insights into individual and combined gene expressions by analyzing millions of normalized scRNA-seq data within the BERT framework. Geneformer (Theodoris et al., 2023) employs a self-supervised masked token prediction objective to decode gene networks, subsequently fine-tuning for chromatin and network dynamics tasks. ScGPT (Cui et al., 2023) benefits from generative pre-training, excelling in functions like cell type annotation, gene perturbation prediction, and pseudo-cell generation. Distinct from foundation models, CHATCELL employs unified sequence generation techniques on single-cell instructions, equipping the model with the ability to accurately follow instructions across various single-cell analysis tasks without the need for pre-training and fine-tuning.

**Instruction-following models.** The inherent strength of LLMs lies in their ability to follow and execute human instructions. Trained on specialized instruction datasets, these models develop a deep understanding of intricate instructions, offering flexibility and a broader scope compared to traditional foundation models. This versatility has led to diverse innovations within biology, such as language-guided molecular design (Edwards et al., 2022; Fang et al., 2024a; Zeng et al., 2023), medical question-answering (Singhal et al., 2023), and automated experimental design (Daniil et al., 2023). The exploration of instruction-following models is emerging as a promising avenue in the single-cell domain. GPTCelltype (Hou and Ji, 2023) explores the feasibility of using GPT-4 for cell type annotation, indicating a new step forward in language-guided single-cell analysis. Cell2sentence (Levine et al., 2023) demonstrates how gene expression profiles can be translated into gene name sequences, illustrating the potential for integrating LLMs into analyzing single-cell data. Apart from them, CHATCELL employs vocabulary adaptation to familiarize LLMs with single-cell terminology and extend their proficiency across a variety of tasks through unified sequence generation. It facilitates a seamless entry for researchers into the field, allowing direct information retrieval through chat and thereby enhancing the accessibility of single-cell analysis.

## 3 Methodology

Figure 2 illustrates the framework of CHATCELL. We detail the conversational architecture of CHATCELL (§ 3.1), transform single-cell data into a cell sentence format compatible with LLMs (§ 3.2), and apply vocabulary adaptation to accommodate single-cell-specific terminology (§ 3.3). Then, we implement unified sequence generation to improve the proficiency of CHATCELL in handling various single-cell analysis tasks (§ 3.4). Table 1 summarizes the principal notations for quick reference.

| Notation | Meaning |
|---|---|
| $X$ | The task description and specific input |
| $Y$ | The target output |
| $\mathrm{M}$ | The language model |
| $\mathbf{C}$ | The cell-by-gene expression matrix |
| $\mathbf{S}$ | The gene sequence or cell sentence |
| $D$ | The number of occurrences of gene $j$ in $\mathbf{S}$ |
| $c_{i,j}$ | The expression value of gene $j$ in cell $i$ |
| $e_j$ | The estimated expression value of gene $j$ in cell $i$, abbreviation of $e_{i,j}$ |

Table 1: Notations and their meanings.

### 3.1 Overview of CHATCELL

CHATCELL is conceived to streamline the analysis and generation of single-cell data within a conversational context. At the core of this paradigm lies an LLM, denoted as $\mathrm{M}$, which has developed a profound understanding of natural language through extensive training on diverse textual corpora. A standard instruction entry provided to $\mathrm{M}$ includes a **task description** that clearly outlines the task at hand, coupled with **input** specifying the conditions, and a **target output** that defines the desired outcome. This process can be formalized as:

$$Y = \mathrm{M}(X). \tag{1}$$

Here, $X$ communicates the specifics and requisites of the task to $\mathrm{M}$, while $Y$ sets an intended objective that guides $\mathrm{M}$ in generating outputs that align with the predefined goals of tasks.

### 3.2 Translation Between scRNA-seq Data and Cell Sentence

In the CHATCELL framework, a crucial step is the conversion of complex scRNA-seq data into a format that is compatible with LLMs. ScRNA-seq data is typically structured into gene expression matrices that provide in-depth insights into the genetic profiles of individual cells. However, the considerable volume and high sparsity of these matrices pose computational and scalability challenges.

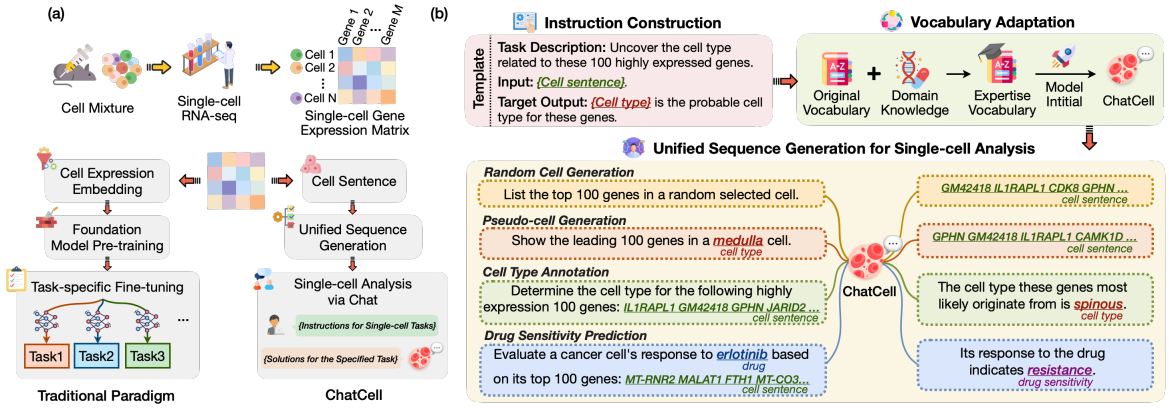


Figure 2: (a) Comparison of traditional single-cell analysis and CHATCELL. (b) Overview of CHATCELL.

We address these challenges by converting scRNA-seq data into a sequence format. Notably, gene expression levels in scRNA-seq data exhibit a log-linear relationship with their rank order, following inverse-rank frequency patterns (Furusawa and Kaneko, 2003; Qiu et al., 2013). This relationship offers an opportunity to simplify complex matrix data into a more manageable form. We define a cell-by-gene expression matrix $\mathbf{C}$, the transpose of the raw gene expression matrix, with each element $c_{i,j}$ representing the observed RNA molecule count of gene $j$ in cell $i$. Inspired by Levine et al. (2023), we transform $\mathbf{C}$ into a sequence of gene names, arranged in descending order of gene expression. This strategy preserves the critical information embedded in the original matrix while rendering the data more tractable for LLM processing. To capture the most significant expression patterns, we prioritize the top 100 most expressed genes, since lower-ranked genes tend to have more consistent expression values.

The reverse process involves reconstructing the gene expression matrix $\mathbf{C}$ from the generated gene sequences $\mathbf{S}$:

$$e_j = a \cdot \log(r_j) + b, \tag{2}$$

where $e_j$ (representing $e_{i,j}$ for simplicity) estimates the expression for gene $j$ in cell $i$, $r_j$ is the rank order, with $a$ and $b$ being the slope and intercept, respectively. When generating cell sentences, duplicates of genes may occur. For the set of duplicates $\{j_1, \ldots, j_D\}$ representing gene $j$, we calculate its average rank $r_j$ as follows:

$$r_j = \frac{1}{D} \sum_{d=1}^{D} \text{rank}(j_d), \tag{3}$$

where $\text{rank}(j_d)$ is the rank of the $d$-th occurrence of gene $j$ in the sentence. Genes absent from $\mathbf{S}$ are assigned an expression level of zero:

$$e_j = \begin{cases} a \cdot \log(r_j) + b, & \text{if } j \in \mathbf{S} \\ 0, & \text{otherwise} \end{cases} \tag{4}$$

Consequently, the expression of gene $j$ in cell $i$ within matrix $\mathbf{C}$, denoted as $c_{i,j}$, can be approximated using the value of $e_j$.

**Algorithm 1** Vocabulary Adaptation

**Input:** Original vocabulary of LLM $\mathcal{V}_{\text{orig}}$, List of gene names $\mathcal{A}$ sorted by descending frequency, List of essential cell biology terms $\mathcal{B}$, Vocabulary size upper bound $\delta$
**Output:** Expanded vocabulary $\mathcal{V}_{\text{final}}$

$\mathcal{V}_{\text{temp}} \leftarrow \mathcal{V}_{\text{orig}}$
**for** $\forall a \in \mathcal{A}$ **do**
  **if** $a \notin \mathcal{V}_{\text{temp}}$ **then**
    $\mathcal{V}_{\text{temp}} \leftarrow \mathcal{V}_{\text{temp}} \cup \{a\}$
    **if** $|\mathcal{V}_{\text{temp}}| \geq \delta$ **then**
      **break**
    **end if**
  **end if**
**end for**
**for** $\forall b \in \mathcal{B}$ **do**
  **if** $b \notin \mathcal{V}_{\text{temp}}$ **then**
    $\mathcal{V}_{\text{temp}} \leftarrow \mathcal{V}_{\text{temp}} \cup \{b\}$
  **end if**
**end for**
**return** $\mathcal{V}_{\text{final}} \leftarrow \mathcal{V}_{\text{tmp}}$

### 3.3 Vocabulary Adaptation for Single-Cell

Effective representation of cell sentences in single-cell analysis demands a vocabulary that fully captures domain-specific terms (Pei et al., 2023). The default vocabularies of pre-trained LLMs often lack the specialized lexicon crucial for interpreting single-cell data, particularly gene names. For example, a gene name like `CAMK1D` could be improperly segmented by standard tokenizers into `CAM`, `K`, `1`, and `D`. Here, `CAM` could be misconstrued as a term unrelated to genes, such as "Computer-Aided Man-

ufacturing", while K might be confused with the chemical symbol of Potassium, and 1 and D become isolated characters, thereby detracting from their contextual significance in genetics.

To bridge this gap, we implement vocabulary adaptation for LLMs, as outlined in Algorithm 1. This algorithm incorporates gene names and essential cell biology terminology, including cell types and drug names, into the LLM's existing vocabulary. Given the unique and complex nature of gene nomenclature, which often strays from standard English word formations, we treat these terms as indivisible entities. Consequently, this adaptation enriches the LLM's lexicon with domain-specific terms and subword units, leveraging domain knowledge to improve its efficacy in single-cell analysis.

### 3.4 Unified Sequence Generation for Single-Cell Analysis

The objective of CHATCELL is to enable researchers to conduct comprehensive single-cell analysis using natural language inputs, ensuring LLM's adeptness in both single-cell and natural language. CHATCELL is built upon an encoder-decoder transformer architecture and treats all tasks as sequence generation problems, facilitating cross-task knowledge sharing. By exposing the model to a wide variety of single-cell analysis tasks, it not only identifies task-specific patterns but also develops a holistic understanding of the entire domain. As illustrated in Figure 2, we focus on four primary tasks: **random cell sentence generation** challenges the model to create cell sentences without predefined biological conditions, **pseudo-cell generation** involves creating gene sequences for specific cell types, **cell type annotation** requires the model to classify cells based on gene expression patterns, and **drug sensitivity prediction** predicts the response of different cells to various drugs. Further details and examples are in Appendix § A.

In real-world scenarios, human communication exhibits inherent diversity and complexity, characterized by a wide array of linguistic styles and expressions. CHATCELL, designed to engage in conversational interactions, must be adept at handling this linguistic variability. For each task, we start with a clear and concise human-written description. This description is then fed into GPT-3.5-turbo, leveraging its capability to produce diverse renditions of the same concept. This diversity in training ensures that CHATCELL learns to understand and respond to different modes of language expression, making it a robust tool for versatile communicative interactions in single-cell analysis.

## 4 Experiments

### 4.1 Experimental Setup

***Baselines.*** The compared baselines (detailed in Appendix § B) include domain-specific models like scVI (Lopez et al., 2018), scDEAL (Chen et al., 2022), Cell2Sentence (Levine et al., 2023), and scBERT (Yang et al., 2022) each specifically designed for single-cell analysis. We also compare our model with generalist models such as Transformer (Vaswani et al., 2017) and GPT-3.5-turbo (OpenAI, 2023).

***Implementation Details.*** CHATCELL is implemented using the PyTorch framework and trained on an Nvidia A800 GPU. We initialize our model using three variants of the T5 architecture as pre-trained foundations, configured with 60M parameters for small, 220M for base, and 770M for large. The training employs the AdamW optimizer, incorporating a weight decay of 0.01. Over a total of 960,000 steps, we maintain a batch size of 8 and set the learning rate to 4e-5. More information about datasets and experimental setup are detailed in Appendix § C and D.

### 4.2 Random Cell Generation

| Model | ↓ Δ Cell Length | ↑ Validity (%) | ↑ Uniqueness (%) |
|---|---|---|---|
| Transformer | 64.75 | 99.97 | 11.23 |
| Cell2Sentence | 0.12 | 94.51 | 99.95 |
| CHATCELL | **0.00** | **100.00** | **100.00** |
| CHATCELL | 0.99 | **100.00** | **100.00** |
| CHATCELL | **0.00** | **100.00** | **100.00** |

Table 2: Performance of random cell generation. The icons, , and indicate small, base, and large configurations, respectively. and signify whether the model is general or domain-specific.

Table 2 demonstrates that across its three configurations, CHATCELL consistently achieves perfect *validity* and *uniqueness* scores for the generated cells, with *cell lengths* closely aligning with the training setting of 100 genes. *Validity* refers to the proportion of generated gene tokens that accurately correspond to real gene names, while *uniqueness* assesses the non-repetition among gene tokens within each cell sentence. The discrepancy in *cell lengths* between the training and generation phases measures the model's capacity to accurately reflect the predefined data structure. While the Transformer model similarly scores high in validity, it

| Model | Quality | | | | | | | | Discriminability | | | | | | | |
|---|---|---|---|---|---|---|---|---|---|---|---|---|---|---|---|---|
| | K = 5 | | K = 10 | | K = 25 | | K = 50 | | K = 5 | | K = 10 | | K = 25 | | K = 50 | |
| | Expr. | Lev. | Expr. | Lev. | Expr. | Lev. | Expr. | Lev. | Expr. | Lev. | Expr. | Lev. | Expr. | Lev. | Expr. | Lev. |
| Transformer | 18.69 | 11.39 | 8.75 | 10.94 | 5.38 | 8.93 | 8.75 | 8.93 | 18.69 | 10.67 | 4.65 | 10.39 | 0.00 | 7.66 | 3.92 | 7.75 |
| scVI | 14.94 | - | 14.39 | - | 14.15 | - | 14.88 | - | 0.34 | - | 0.24 | - | 0.27 | - | 9.75 | - |
| Cell2Sentence | 57.52 | 25.43 | 60.44 | 30.99 | 61.26 | 38.20 | 61.17 | 38.47 | 50.68 | 22.15 | 54.06 | 24.70 | 56.34 | 30.26 | 56.43 | 29.44 |
| CHATCELL | 35.28 | 22.15 | 36.19 | 26.44 | 37.10 | 30.99 | 35.10 | 31.72 | 29.44 | 18.41 | 31.72 | 21.06 | 34.46 | 24.25 | 32.18 | 24.25 |
| CHATCELL | 62.90 | 27.71 | 66.55 | 35.37 | 70.37 | 40.29 | 70.01 | 42.11 | 61.35 | 23.97 | 64.45 | 28.35 | 67.55 | 29.90 | 65.36 | 28.35 |
| CHATCELL | **74.20** | **49.23** | **76.94** | **49.77** | **77.94** | **50.87** | **77.58** | **49.13** | **72.11** | **40.38** | **74.84** | **38.56** | **74.84** | **37.01** | **74.11** | **35.55** |

Table 3: Performance (%) of pseudo-cell generation. KNN classification is performed in both the cell sentence space utilizing Levenshtein distance (Lev.) and in the expression vectors (Expr.) after reconversion.

falls short in uniqueness due to repeated gene tokens and tends to generate cell sentences exceeding the optimal length. Cell2Sentence exhibits similar uniqueness but slightly lower validity. These comparisons highlight CHATCELL's strength to produce both diverse and biologically plausible gene sequences, demonstrating its potential to simulate real single-cell data.

### 4.3 Pseudo-cell Generation

When given specific cell types, we evaluate the performance of the generated cells through k-Nearest Neighbors (KNN) accuracy. *Quality* assesses how closely the generated cell types align with their nearest neighbors in the actual dataset, serving as a measure of the model's precision in simulating real cells. *Discriminability* evaluates how well the model can distinguish between different cell types when satisfying *quality*, by classifying each generated cell based on the cell types of its nearest neighbors within both the actual and generated datasets. Table 3 presents the KNN accuracy of each model across varying numbers of neighbors. CHATCELL surpasses traditional models, including scVI, a probabilistic generative model for single-cell data utilizing variational inference, highlighting the potential superiority of language model-based approaches in grasping cellular complexities. Beyond generating cells that accurately match specific cell types, CHATCELL adeptly clusters cells of the same type together and clearly delineates different types from each other. This capability is crucial for accurately simulating real biological systems, particularly in capturing the complexities of tumor heterogeneity.

### 4.4 Cell Type Annotation

CHATCELL revolutionizes cell type annotation by eliminating the need for classifier training. Instead, task descriptions and cell sentences are fed directly as instructions into the model, which then predicts the cell type through a sequence generation manner. Table 4 reveals that CHATCELL holds a distinct edge over competing models, reflecting its proficiency in deciphering complex relationships between gene expressions and corresponding cell types. While GPT-3.5-turbo shows robust capabilities for general language processing, it falls short in parsing the specialized terminology central to single-cell data. Furthermore, the performance of both Transformers and Cell2Sentence trails behind CHATCELL, despite incorporating domain-specific data. This emphasizes that a true understanding of single-cell intricacies goes beyond general language competencies, necessitating a more suitable architecture coupled with the adaptability to the specific vocabulary of single-cell data.

| Model | Accuracy | F1 | Precision | Recall |
|---|---|---|---|---|
| Transformer | 37.35 | 35.26 | 37.52 | 37.35 |
| GPT-3.5-turbo | 11.09 | 8.88 | 9.99 | 11.09 |
| Cell2Sentence | 67.85 | 67.92 | 68.87 | 67.85 |
| CHATCELL | 68.20 | 67.23 | 67.72 | 68.20 |
| CHATCELL | 77.82 | 77.76 | 78.08 | 77.82 |
| CHATCELL | **81.63** | **81.51** | **81.71** | **81.63** |

Table 4: Performance (%) of cell type annotation.

### 4.5 Drug Sensitivity Prediction

Similarly, the task of drug sensitivity prediction is also accomplished in an autoregressive manner, obviating the need for a distinct classifier. As shown in Table 5, experiments are conducted on two drug response datasets. CHATCELL outperforms in both the GSE149383 and GSE117872 datasets, surpassing the specialized model scDEAL and achieving performance levels comparable to the single-cell foundation model scBERT. Intriguingly, GPT-3.5-turbo, despite being a general-purpose model, even surpasses scDEAL in performance on both datasets. This indicates an increasing competitiveness of general-purpose models in specialized tasks. Enhanced with targeted vocabulary adaptation and instruction tuning, CHATCELL further excels, showcasing the strength of combining advanced language model capabilities with specific

| Model | GSE149383 | | | | GSE117872 | | | |
|---|---|---|---|---|---|---|---|---|
| | Accuracy | F1 | Precision | Recall | Accuracy | F1 | Precision | Recall |
| Transformer | 63.64 | 61.65 | 65.60 | 63.64 | 69.47 | 70.61 | 73.76 | 69.47 |
| GPT-3.5-turbo | 48.73 | 47.39 | 49.54 | 48.73 | 63.36 | 64.23 | 65.54 | 63.36 |
| scDEAL | 45.82 | 43.53 | 44.09 | 45.82 | 47.33 | 49.56 | 54.50 | 47.33 |
| scBERT | **97.82** | **97.82** | **97.86** | **97.82** | 98.47 | 98.17 | 98.47 | 98.47 |
| CHATCELL | 93.45 | 93.45 | 93.48 | 93.45 | 96.18 | 96.17 | 96.17 | 96.18 |
| CHATCELL | 95.27 | 95.28 | 95.40 | 95.27 | 97.71 | 98.08 | 98.49 | 97.71 |
| CHATCELL | **97.82** | **97.82** | 97.83 | **97.82** | **99.24** | **99.23** | **99.24** | **99.24** |

Table 5: Performance (%) of drug sensitivity prediction on two datasets.

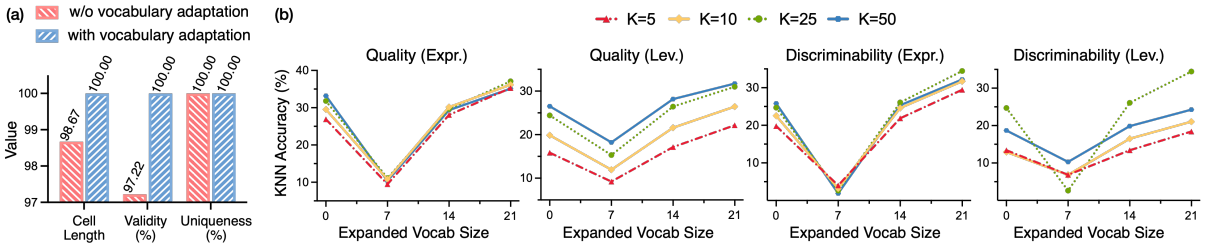


Figure 3: Performance variations in (a) random cell generation and (b) pseudo-cell generation across different expanded vocabulary sizes (in thousands).

task-focused refinements.

## 5 Further Analysis

**Richer vocabulary enhances single-cell interpretation and generation.** To identify the optimal balance between vocabulary richness and computational efficiency, we conduct an ablation study on two cell generation tasks, as depicted in Figure 3. For random cell generation, we observe that vocabulary expansion consistently improves the generation of valid and ideally lengthed cell sentences, regardless of the extent of the increase. However, uniqueness remains largely unaffected by the expansion, consistently nearing 100%. For pseudo-cell generation, introducing 7,000 gene names initially leads to a performance dip, possibly as the partial vocabulary expansion introduces ambiguity. Performance improves as the vocabulary expands to 14,000 gene names and continues to rise until reaching optimal levels at a 21,000 gene name threshold. At this point, the model is equipped with an extensive set of single-cell terminologies, enabling it to accurately understand and handle the intricate relationships within single-cell data.

**Vocabulary adaptation improves domain-specific language understanding.** To further investigate vocabulary adaptation's effect, we use t-SNE to visualize general versus domain-specific word embeddings before and after training, shown in Figure 4. Initially, embeddings overlap significantly. After training, domain-specific words begin to form discrete clusters, evidenced

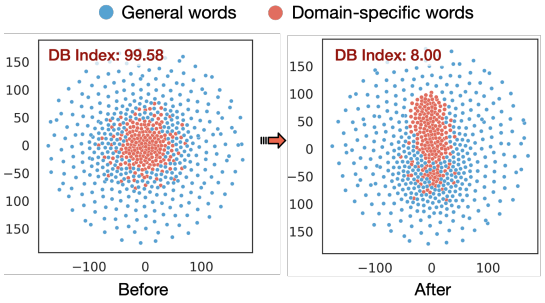


Figure 4: Visualization of word embeddings before and after training. A lower DB index indicates better clustering separation.

by a lower Davies-Bouldin (DB) index, indicating better clustering. This implies that the embeddings of these words have become more representative of their specific meanings and contexts within their respective domains, rather than remaining ambiguously intermingled with general words. In contrast, general word embeddings remain largely unchanged, highlighting the precision of our vocabulary adaptation strategy in bolstering domain expertise without compromising general language processing.

**CHATCELL demonstrates robustness to novel phrasing.** Given the diversity of human expression, maintaining robust performance across variously phrased instructions is essential for a chat model. Hence, we replace all task descriptions in the test set with variations that the model has not previously encountered during training or validation, to assess its proficiency with unseen instructions. Figure 5 illustrates the results for the drug

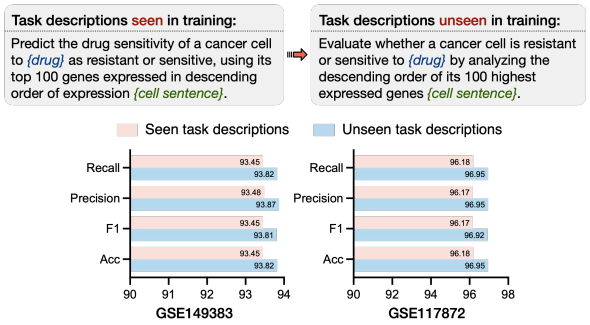


Figure 5: Performance (%) comparison of drug sensitivity prediction using task descriptions seen or unseen during training.

sensitivity prediction. Despite the novel phrasing of instructions, the model's performance remains almost unchanged. This highlights the model's robustness and generalization ability, effectively handling tasks with varied descriptions and enhancing conversational single-cell analysis.

**CHATCELL accurately captures cell type characteristics in generation.** To assess the biological accuracy of cell sentences generated by CHATCELL, we visualize their corresponding gene expression matrices in two dimensions, following the pseudo-cell generation experimental setting. Figure 6 (a) shows that cell distributions generated by CHATCELL closely resemble those of real cells, confirmed by Maximum Mean Discrepancy (MMD). The distinct clustering of cell types in the generated data demonstrates CHATCELL's ability to capture and differentiate unique cell characteristics, indicating its capacity to generate detailed profiles for each cell type.

**CHATCELL uncovers gene-level biological insights.** Each cell sentence is composed of genes. To delve into the biological significance of the representations learned at a finer granularity, we analyze gene associations based on their embeddings obtained by CHATCELL. We employ $K$-means clustering to categorize genes, grouping those with high associations, as depicted in Figure 6 (b). For each cluster, we further conduct gene pathway enrichment analysis (Aleksander et al., 2023). This analysis, which focuses on a series of interconnected biochemical reactions working together to perform specific biological functions like energy production or cell growth, offers insights into the biological processes each cluster is involved in. Specifically, we map these genes to their related pathways in the Gene Ontology (Ashburner et al., 2000) to identify the biological pathways significantly associated with them, with the significance of these associations quantified by $p$-values, as illustrated in Appendix Figure 8. As illustrated, genes in cluster 1 are linked to tissue structure regulation, while those in cluster 2 are predominantly related to the immune system, inflammatory responses, and cell signaling. Cluster 3 encompasses genes associated with immune cell activation and signaling, cluster 4 with leukocyte functions and immune responses, and cluster 5 primarily with tissue development. The distinct separation of these gene clusters further demonstrates CHATCELL's effective capture of intricate relationships between genes and their functions, validating its profound understanding of complex biological processes.

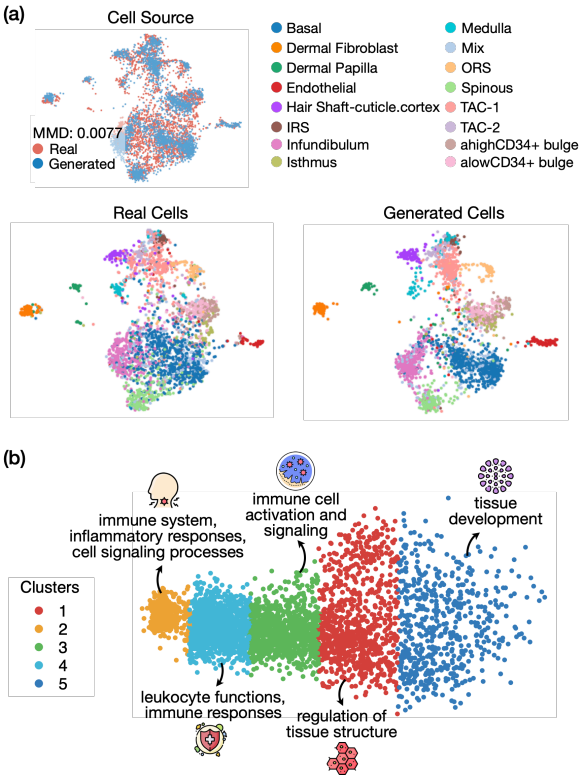


Figure 6: (a) Distribution of real cells and generated cells. (b) Gene clusters and their associated pathways.

## 6 Conclusion and Future Work

In this work, we propose CHATCELL, a framework that facilitates single-cell analysis with natural language. Our in-depth study on CHATCELL confirms its proficiency in deciphering complex single-cell data and its versatility across a wide range of analysis tasks. Interesting future directions include: *i)* integrating multimodal data like gene expression with proteomics, *ii)* applying CHATCELL in personalized medicine to tailor drug treatments. We make our pre-trained model, code, and data pub-

licly available, in the hope that our work will foster future research in the field.

## Limitations

As an initial attempt to revolutionize single-cell analysis, CHATCELL encounters several limitations that warrant attention for future improvement:

**Task coverage and data diversity.** CHATCELL does not span all tasks or capture the full variety of single-cell data. For example, the drug types explored do not cover all possible reactions across different cancer types or therapeutic conditions. This limitation may restrict the applicability of our findings to a wider array of biological questions and clinical scenarios.

**Representation of single-cell language.** By representing gene expression matrices as cell sentences sorted by expression levels and limiting the length to 100, there might be inherent limitations. This simplification might overlook the complexity and nuances of cellular states and interactions, possibly impacting the accuracy and depth of analysis. The arbitrary cutoff could exclude relevant genes and interactions, limiting the model's ability to capture the full biological context.

**Model scale.** The optimal scale of the model for this specific domain remains an open question. While larger models in other fields offer enhanced capabilities for processing complex datasets, the efficiency and specificity of smaller models cannot be overlooked. This uncertainty highlights the need for more research to find the right balance between computational demands and the depth of analysis.

**Data modality.** CHATCELL primarily focuses on single modality information, mainly gene expression data, neglecting the potential insights that could be gained from integrating multiple data types. The complex nature of single-cell biology often requires a multi-modal approach to fully understand the intricacies of cellular functions, interactions, and responses to different conditions.

## Ethical Considerations

Our experiments and model training exclusively utilize publicly available datasets (as detailed in Appendix C), avoiding ethical concerns related to privacy, confidentiality, or misuse of personal biological information.

## References


Alexandre F Aissa, Abul BMMK Islam, Majd M Ariss, Cammille C Go, Alexandra E Rader, Ryan D Conrardy, Alexa M Gajda, Carlota Rubio-Perez, Klara Valyi-Nagy, Mary Pasquinelli, et al. 2021. Single-cell transcriptional changes associated with drug tolerance and response to combination therapies in cancer. *Nature communications*, 12(1):1628.

Suzi A Aleksander, James Balhoff, Seth Carbon, J Michael Cherry, Harold J Drabkin, Dustin Ebert, Marc Feuermann, Pascale Gaudet, Nomi L Harris, et al. 2023. The gene ontology knowledgebase in 2023. *Genetics*, 224(1):iyad031.

Philipp Angerer, Lukas Simon, Sophie Tritschler, F Alexander Wolf, David Fischer, and Fabian J Theis. 2017. Single cells make big data: new challenges and opportunities in transcriptomics. *Current opinion in systems biology*, 4:85–91.

Michael Ashburner, Catherine A Ball, Judith A Blake, David Botstein, Heather Butler, J Michael Cherry, Allan P Davis, Kara Dolinski, Selina S Dwight, Janan T Eppig, et al. 2000. Gene ontology: tool for the unification of biology. *Nature genetics*, 25(1):25–29.

Tanya Barrett, Stephen E Wilhite, Pierre Ledoux, Carlos Evangelista, Irene F Kim, Maxim Tomashevsky, Kimberly A Marshall, Katherine H Phillippy, Patti M Sherman, Michelle Holko, et al. 2012. Ncbi geo: archive for functional genomics data sets—update. *Nucleic acids research*, 41(D1):D991–D995.

William Bechtel. 2006. *Discovering cell mechanisms: The creation of modern cell biology*. Cambridge University Press.

Gerard A Bouland, Ahmed Mahfouz, and Marcel JT Reinders. 2023. Consequences and opportunities arising due to sparser single-cell rna-seq datasets. *Genome biology*, 24(1):86.

Alvis Brazma and Jaak Vilo. 2000. Gene expression data analysis. *FEBS letters*, 480(1):17–24.

Junyue Cao, Malte Spielmann, Xiaojie Qiu, Xingfan Huang, Daniel M Ibrahim, Andrew J Hill, Fan Zhang, Stefan Mundlos, Lena Christiansen, Frank J Steemers, et al. 2019. The single-cell transcriptional landscape of mammalian organogenesis. *Nature*, 566(7745):496–502.

Junyi Chen, Xiaoying Wang, Anjun Ma, Qi-En Wang, Bingqiang Liu, Lang Li, Dong Xu, and Qin Ma. 2022. Deep transfer learning of cancer drug responses by integrating bulk and single-cell rna-seq data. *Nature Communications*, 13(1):6494.

Haotian Cui, Chloe Wang, Hassaan Maan, Kuan Pang, Fengning Luo, and Bo Wang. 2023. scgpt: Towards building a foundation model for single-cell multi-omics using generative ai. *bioRxiv*, pages 2023–04.

A. Boiko Daniil, MacKnight Robert, Kline Ben, and Gomes Gabe. 2023. Autonomous chemical research with large language models. *Nature*, pages 570–578.

Jonas Degrave, Federico Felici, Jonas Buchli, Michael Neunert, Brendan Tracey, Francesco Carpanese, Timo Ewalds, Roland Hafner, Abbas Abdolmaleki, Diego de Las Casas, et al. 2022. Magnetic control of tokamak plasmas through deep reinforcement learning. *Nature*, 602(7897):414–419.

Jacob Devlin, Ming-Wei Chang, Kenton Lee, and Kristina Toutanova. 2019. BERT: pre-training of deep bidirectional transformers for language understanding. In *NAACL-HLT (1)*, pages 4171–4186. Association for Computational Linguistics.

Carl Edwards, Tuan Lai, Kevin Ros, Garrett Honke, Kyunghyun Cho, and Heng Ji. 2022. Translation between molecules and natural language. In *Proceedings of the 2022 Conference on Empirical Methods in Natural Language Processing*, pages 375–413, Abu Dhabi, United Arab Emirates. Association for Computational Linguistics.

Yin Fang, Xiaozhuan Liang, Ningyu Zhang, Kangwei Liu, Rui Huang, Zhuo Chen, Xiaohui Fan, and Huajun Chen. 2024a. Mol-instructions: A large-scale biomolecular instruction dataset for large language models. *ICLR*.

Yin Fang, Ningyu Zhang, Zhuo Chen, Xiaohui Fan, and Huajun Chen. 2024b. Domain-agnostic molecular generation with self-feedback. *ICLR*, abs/2301.11259.

Chikara Furusawa and Kunihiko Kaneko. 2003. Zipf's law in gene expression. *Physical review letters*, 90(8):088102.

Wenpin Hou and Zhicheng Ji. 2023. Reference-free and cost-effective automated cell type annotation with gpt-4 in single-cell rna-seq analysis. *bioRxiv*, pages 2023–04.

Yuge Ji, Mohammad Lotfollahi, F Alexander Wolf, and Fabian J Theis. 2021. Machine learning for perturbational single-cell omics. *Cell Systems*, 12(6):522–537.

John Jumper, Richard Evans, Alexander Pritzel, Tim Green, Michael Figurnov, Olaf Ronneberger, Kathryn Tunyasuvunakool, Russ Bates, Augustin Žídek, Anna Potapenko, et al. 2021. Highly accurate protein structure prediction with alphafold. *Nature*, 596(7873):583–589.

Daniel Levine, Syed Asad Rizvi, Sacha Lévy, Nazreen Pallikkavaliyaveetil, Ruiming Wu, Insu Han, Zihe Zheng, Antonio Henrique de Oliveira Fonseca, Xingyu Chen, Sina Ghadermarzi, et al. 2023. Cell2sentence: Teaching large language models the language of biology. *bioRxiv*, pages 2023–09.

Mike Lewis, Yinhan Liu, Naman Goyal, Marjan Ghazvininejad, Abdelrahman Mohamed, Omer Levy, Veselin Stoyanov, and Luke Zettlemoyer. 2020. BART: denoising sequence-to-sequence pre-training for natural language generation, translation, and comprehension. In *ACL*, pages 7871–7880. Association for Computational Linguistics.

Jie Liao, Jingyang Qian, Yin Fang, Zhuo Chen, Xiang Zhuang, Ningyu Zhang, Xin Shao, Yining Hu, Penghui Yang, Junyun Cheng, et al. 2022. De novo analysis of bulk rna-seq data at spatially resolved single-cell resolution. *Nature Communications*, 13(1):6498.

Yuval Lieberman, Lior Rokach, and Tal Shay. 2018. Castle–classification of single cells by transfer learning: harnessing the power of publicly available single cell rna sequencing experiments to annotate new experiments. *PloS one*, 13(10):e0205499.

Jiajia Liu, Zhiwei Fan, Weiling Zhao, and Xiaobo Zhou. 2021. Machine intelligence in single-cell data analysis: advances and new challenges. *Frontiers in Genetics*, 12:655536.

Romain Lopez, Jeffrey Regier, Michael B Cole, Michael I Jordan, and Nir Yosef. 2018. Deep generative modeling for single-cell transcriptomics. *Nature methods*, 15(12):1053–1058.

Sai Ma, Bing Zhang, Lindsay M LaFave, Andrew S Earl, Zachary Chiang, Yan Hu, Jiarui Ding, Alison Brack, Vinay K Kartha, Tristan Tay, et al. 2020. Chromatin potential identified by shared single-cell profiling of rna and chromatin. *Cell*, 183(4):1103–1116.

Shentong Mo, Xi Fu, Chenyang Hong, Yizhen Chen, Yuxuan Zheng, Xiangru Tang, Zhiqiang Shen, Eric P Xing, and Yanyan Lan. 2021. Multi-modal self-supervised pre-training for regulatory genome across cell types. *arXiv preprint arXiv:2110.05231*.

Sergio Oller-Moreno, Karin Kloiber, Pierre Machart, and Stefan Bonn. 2021. Algorithmic advances in machine learning for single-cell expression analysis. *Current Opinion in Systems Biology*, 25:27–33.

OpenAI. 2023. Gpt-3.5-turbo. https://platform.openai.com/docs/models/gpt-3.5-turbo.

Qizhi Pei, Wei Zhang, Jinhua Zhu, Kehan Wu, Kaiyuan Gao, Lijun Wu, Yingce Xia, and Rui Yan. 2023. Biot5: Enriching cross-modal integration in biology with chemical knowledge and natural language associations. In *EMNLP*, pages 1102–1123. Association for Computational Linguistics.

Mireya Plass, Jordi Solana, F Alexander Wolf, Salah Ayoub, Aristotelis Misios, Petar Glažar, Benedikt Obermayer, Fabian J Theis, Christine Kocks, and Nikolaus Rajewsky. 2018. Cell type atlas and lineage tree of a whole complex animal by single-cell transcriptomics. *Science*, 360(6391):eaaq1723.

Thomas D Pollard, William C Earnshaw, Jennifer Lippincott-Schwartz, and Graham Johnson. 2022. *Cell biology E-book*. Elsevier Health Sciences.

Xing Qiu, Hulin Wu, and Rui Hu. 2013. The impact of quantile and rank normalization procedures on the testing power of gene differential expression analysis. *BMC bioinformatics*, 14:1–10.

Andrea Ravasio, Myint Z Myaing, Shumei Chia, Aditya Arora, Aneesh Sathe, Elaine Yiqun Cao, Cristina Bertocchi, Ankur Sharma, Bakya Arasi, Vin Yee Chung, et al. 2020. Single-cell analysis of epha clustering phenotypes to probe cancer cell heterogeneity. *Communications Biology*, 3(1):429.

Aviv Regev, Sarah A Teichmann, Eric S Lander, Ido Amit, Christophe Benoist, Ewan Birney, Bernd Bodenmiller, Peter Campbell, Piero Carninci, Menna Clatworthy, et al. 2017. The human cell atlas. *elife*, 6:e27041.

Xin Shao, Haihong Yang, Xiang Zhuang, Jie Liao, Penghui Yang, Junyun Cheng, Xiaoyan Lu, Huajun Chen, and Xiaohui Fan. 2021. scdeepsort: a pretrained cell-type annotation method for single-cell transcriptomics using deep learning with a weighted graph neural network. *Nucleic acids research*, 49(21):e122–e122.

Ankur Sharma, Elaine Yiqun Cao, Vibhor Kumar, Xiaoqian Zhang, Hui Sun Leong, Angeline Mei Lin Wong, Neeraja Ramakrishnan, Muhammad Hakimullah, Hui Min Vivian Teo, Fui Teen Chong, et al. 2018. Longitudinal single-cell rna sequencing of patient-derived primary cells reveals drug-induced infidelity in stem cell hierarchy. *Nature communications*, 9(1):4931.

Karan Singhal, Shekoofeh Azizi, Tao Tu, S Sara Mahdavi, Jason Wei, Hyung Won Chung, Nathan Scales, Ajay Tanwani, Heather Cole-Lewis, Stephen Pfohl, et al. 2023. Large language models encode clinical knowledge. *Nature*, 620(7972):172–180.

Chayaporn Suphavilai, Shumei Chia, Ankur Sharma, Lorna Tu, Rafael Peres Da Silva, Aanchal Mongia, Ramanuj DasGupta, and Niranjan Nagarajan. 2021. Predicting heterogeneity in clone-specific therapeutic vulnerabilities using single-cell transcriptomic signatures. *Genome Medicine*, 13(1):1–14.

Alejandro Tejada-Lapuerta, Paul Bertin, Stefan Bauer, Hananeh Aliee, Yoshua Bengio, and Fabian J Theis. 2023. Causal machine learning for single-cell genomics. *arXiv preprint arXiv:2310.14935*.

Christina V Theodoris, Ling Xiao, Anant Chopra, Mark D Chaffin, Zeina R Al Sayed, Matthew C Hill, Helene Mantineo, Elizabeth M Brydon, Zexian Zeng, X Shirley Liu, et al. 2023. Transfer learning enables predictions in network biology. *Nature*, pages 1–9.

Robert Tinn, Hao Cheng, Yu Gu, Naoto Usuyama, Xiaodong Liu, Tristan Naumann, Jianfeng Gao, and Hoifung Poon. 2023. Fine-tuning large neural language models for biomedical natural language processing. *Patterns*, 4(4).

Yaojun Tong and Lixin Zhang. 2023. Discovering the next decade's synthetic biology research trends with chatgpt. *Synthetic and Systems Biotechnology*, 8(2):220.

Ashish Vaswani, Noam Shazeer, Niki Parmar, Jakob Uszkoreit, Llion Jones, Aidan N Gomez, Łukasz Kaiser, and Illia Polosukhin. 2017. Attention is all you need. *Advances in neural information processing systems*, 30.

Hanchen Wang, Tianfan Fu, Yuanqi Du, Wenhao Gao, Kexin Huang, Ziming Liu, Payal Chandak, Shengchao Liu, Peter Van Katwyk, Andreea Deac, et al. 2023. Scientific discovery in the age of artificial intelligence. *Nature*, 620(7972):47–60.

F Alexander Wolf, Philipp Angerer, and Fabian J Theis. 2018. Scanpy: large-scale single-cell gene expression data analysis. *Genome biology*, 19:1–5.

Yan Wu and Kun Zhang. 2020. Tools for the analysis of high-dimensional single-cell rna sequencing data. *Nature Reviews Nephrology*, 16(7):408–421.

Fan Yang, Wenchuan Wang, Fang Wang, Yuan Fang, Duyu Tang, Junzhou Huang, Hui Lu, and Jianhua Yao. 2022. scbert as a large-scale pretrained deep language model for cell type annotation of single-cell rna-seq data. *Nature Machine Intelligence*, 4(10):852–866.

Zheni Zeng, Bangchen Yin, Shipeng Wang, Jiarui Liu, Cheng Yang, Haishen Yao, Xingzhi Sun, Maosong Sun, Guotong Xie, and Zhiyuan Liu. 2023. Interactive molecular discovery with natural language. *CoRR*, abs/2306.11976.

Jinlu Zhang, Yin Fang, Xin Shao, Huajun Chen, Ningyu Zhang, and Xiaohui Fan. 2024. The future of molecular studies through the lens of large language models. *Journal of Chemical Information and Modeling*.

Suyuan Zhao, Jiahuan Zhang, and Zaiqing Nie. 2023. Large-scale cell representation learning via divide-and-conquer contrastive learning. *CoRR*, abs/2306.04371.

Yizhen Zheng, Huan Yee Koh, Jiaxin Ju, Anh T. N. Nguyen, Lauren T. May, Geoffrey I. Webb, and Shirui Pan. 2023. Large language models for scientific synthesis, inference and explanation. *CoRR*, abs/2310.07984.

## A Single-cell Analysis Tasks

We focus on the following single-cell tasks outlined, with detailed examples provided in Figure 9.

***Random Cell Sentence Generation.*** Random cell sentence generation challenges the model to

create cell sentences devoid of predefined biological conditions or constraints. Given a prompt $X$, the model is instructed to generate a cell sentence at random. The target $Y$ is a cell sentence that outlines a plausible gene expression profile, although generated without specific guidance. This task aims to evaluate the model's ability to generate valid and contextually appropriate cell sentences, potentially simulating natural variations in cellular behavior.

***Pseudo-cell Generation.*** Pseudo-cell generation focuses on generating gene sequences tailored to specific cell type labels. The prompt $X$ requests the model to construct a cell sentence for a given cell type, and the target $Y$ is expected to be a cell sentence accurately representing the gene expression profile of that cell type. This task is vital for unraveling gene expression and regulation across different cell types, offering insights for medical research and disease studies, particularly in the context of diseased cell types.

***Cell Type Annotation.*** For cell type annotation, the model is tasked with precisely classifying cells into their respective types based on gene expression patterns encapsulated in cell sentences. Here, the prompt $X$ involves providing a gene sequence for the model to determine the cell type, with the target $Y$ being the accurate identification and classification of that cell type. This task is fundamental for understanding cellular functions and interactions within tissues and organs, playing a crucial role in developmental biology and regenerative medicine.

***Drug Sensitivity Prediction.*** The drug sensitivity prediction task aims to predict the response of different cells to various drugs. In this task, the prompt $X$ presents a cell sentence along with a specific drug, and the model is tasked with predicting the cell's response to the drug. The target $Y$ is an accurate prediction of the cell's sensitivity or resistance to the drug. It is pivotal in designing effective, personalized treatment plans and contributes significantly to drug development, especially in optimizing drug efficacy and safety.

## B Compared Baselines

We compare ChatCell against several baselines in our experiments, 🎓 and 👤 signify whether the model is domain-specific or generalistic:

- 🎓 scVI (Lopez et al., 2018) utilizes a hierarchical Bayesian model, encoding cell transcriptomes into low-dimensional latent vectors, which are then decoded to estimate gene distributional parameters for each cell.
- 🎓 scDEAL (Chen et al., 2022) employs a domain-adaptive neural network for predicting drug responses, aligning bulk–single-cell and gene–drug response relations, and applying the trained model to scRNA-seq data for single-cell drug response predictions.
- 🎓 scBERT (Yang et al., 2022) is a pre-trained model based on the transformer architecture, focusing on gene-gene interactions from scRNA-seq data, followed by fine-tuning for cell type annotation tasks.
- 🎓 Cell2Sentence (Levine et al., 2023) translates single-cell data into a textual format, leveraging LLMs for transcriptomic analysis.
- 👤 Transformer (Vaswani et al., 2017) introduces an architecture based on self-attention mechanisms, setting a standard for various NLP tasks with its ability to handle sequences of data efficiently.
- 👤 GPT-3.5-turbo (OpenAI, 2023) represents an advanced iteration of the Generative Pre-trained Transformer series, offering state-of-the-art performance in generating human-like text, which demonstrates significant potential in understanding and generating complex biological text data.

## C Datasets

For tasks such as random cell sentence generation, pseudo-cell generation, and cell type annotation, we utilize 34,500 cells from the SHARE-seq mouse skin dataset (Ma et al., 2020), including their corresponding cell types, for subsequent processing. For the drug sensitivity prediction task, we select two datasets: GSE149383 (Aissa et al., 2021) records the response of 2,739 human lung cancer cells to the drug Erlotinib, and GSE117872 (Sharma et al., 2018; Ravasio et al., 2020; Suphavilai et al., 2021) records the response of 1,302 human oral squamous cancer cells to the drug Cisplatin. The collected single-cell data are normalized and converted into cell sentences as outlined in § 3.2. To meet the specific requirements of each task, we enrich each single-cell data entry with diverse task descriptions as prompts, transforming them into instructions as described in § 3.4. All these instructions are split into train/validation/test datasets in an 8:1:1 ratio.

# D Experiment Details

## D.1 Data Pre-processing

Standard pre-processing of gene expression matrix $\mathbf{C}$ includes filtering cells and genes with low expression, as well as cells exhibiting high mitochondrial gene counts (Levine et al., 2023). The matrix $\mathbf{C}$ then undergoes row normalization to a total of 10,000 transcript counts per cell, followed by log-normalization:

$$c'_{i,j} = \log_{10}\left(1 + 10^4 \times \frac{c_{i,j}}{\sum_{j=1}^{k} C_{i,k}}\right). \quad (5)$$

Furthermore, our dataset includes single-cell data from both mice and humans. For consistency, all gene names for cell types are represented in uppercase (e.g., "MALAT-1" for metastasis-associated lung adenocarcinoma transcript 1 in both humans and mice). Since scBERT is pre-trained on human single-cell data and can not transfer effectively to mouse data, it is not selected as a baseline for the cell type annotation task. This highlights our model's adaptability and applicability to both mouse and human single-cell data.

## D.2 Baseline Reproduction

In our experiments, we reproduce all baseline models using their open-source codes, ensuring identical experimental conditions are maintained. Specifically, scVI, scDEAL, Transformer, and Cell2Sentence are trained from scratch on our training set, while scBERT undergoes fine-tuning based on pre-existing foundation model weights. GPT-3.5-turbo is accessed through its API.

## D.3 Inference

During batch inference, the hyperparameters are set as follows:

| Hyper-parameters | Value |
|---|---|
| Top-p | 0.95 |
| Top-k | 50 |
| Max-length | 512 |
| No-repeat-ngram-size | 2 |

Table 6: Hyper-parameter settings in batch inference.

## D.4 Main Results

For pseudo-cell generation experiments, KNN classification requires cell types to have at least 500 samples in the training dataset, ensuring a sufficient number of samples per cell type for meaningful comparisons, leading to the selection of 16 cell types for experimentation. For the cell type annotation and drug sensitivity prediction tasks, weighted F1 scores, recall, and precision are used as evaluation metrics.

## D.5 Further Analysis

In § 5, we utilize models configured with the small setting for Figures 3 and 5, and the base setting for Figures 4 and 6.

During the vocabulary visualization experiment (Figures 4), we sample 100-200 words from the embedding layer for visualization purposes. This approach is adopted because displaying the full vocabulary results in overly dense images, which are not conducive to observation.

# E Additional Results

Figure 7 complements Figure 5 by displaying the model's robustness to seen and unseen task descriptions under both base and large configurations. This demonstrates CHATCELL's essential chat model capability to handle diverse expressions of task descriptions.

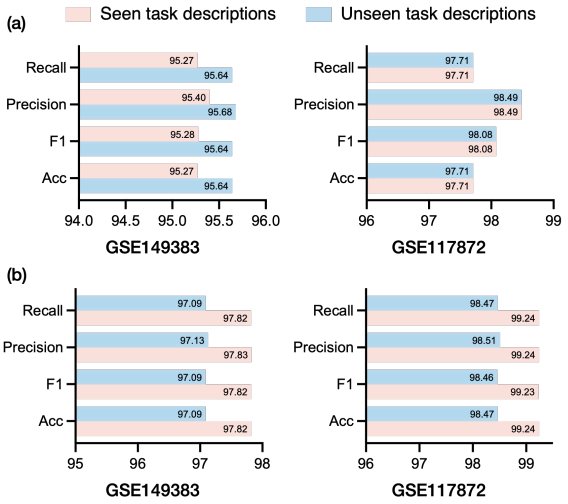


Figure 7: Performance (%) comparison of drug sensitivity prediction using task descriptions seen or unseen during training under base (a) and large (b) configurations.

Meanwhile, Figure 8 provides a detailed expansion of Figure 6 (b), showing each gene cluster and its most associated pathways. This proves CHATCELL's ability to capture the relationships between genes and their functions, thereby enhancing its comprehension of biological processes.

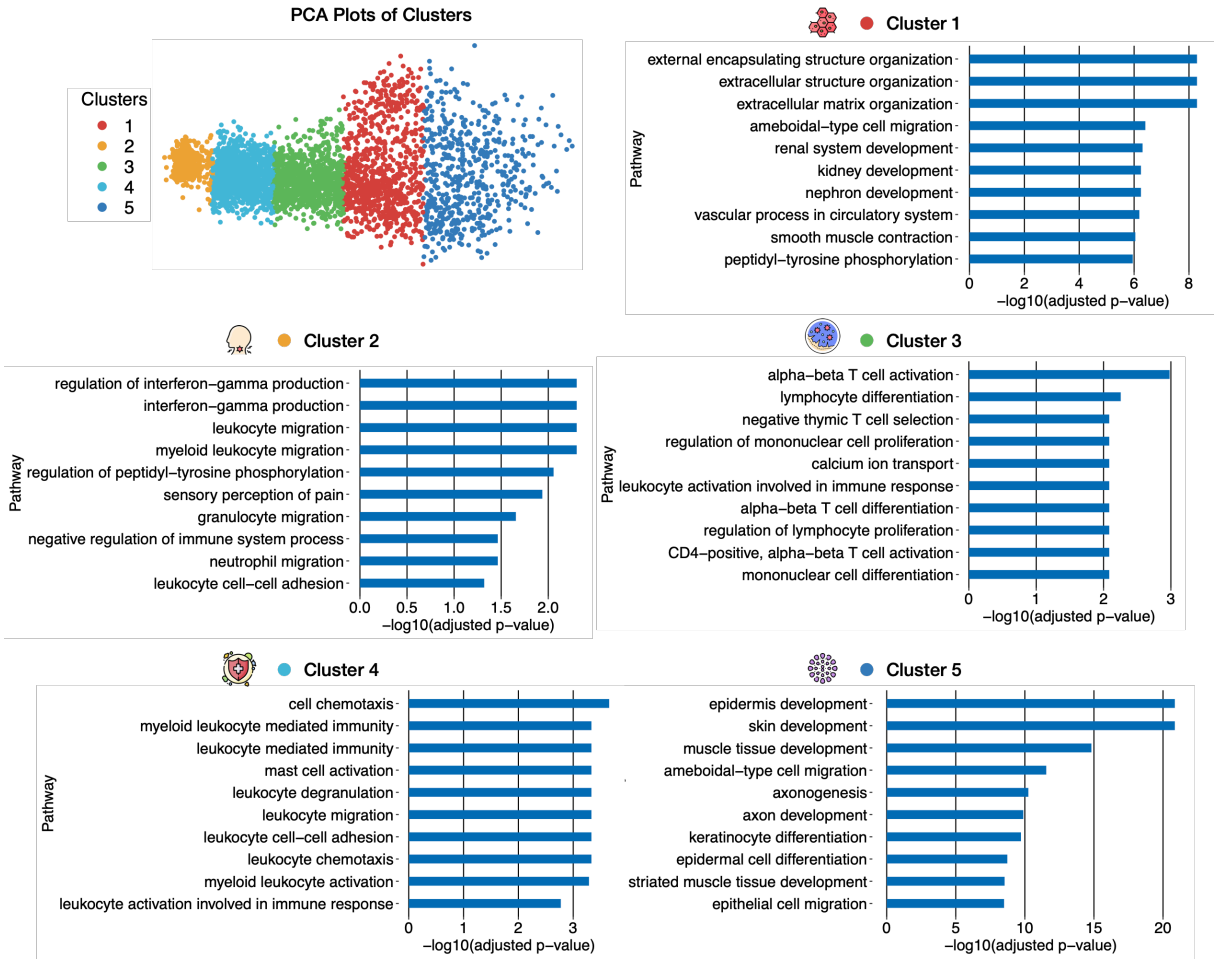


Figure 8: Gene pathway enrichment analysis. Genes are mapped to their corresponding biological pathways, with the significance of these associations quantified using $p$-values.

**Random Cell Generation**
**Source:** Show the 100 primary genes for a cell, sorted by decreasing expression:

**Target:** IL1RAPL1 GM42418 GPHN MALAT1 JARID2 CDK8 CAMK1D FGFR2 LARS2 ZC3H7A MYOF BARX2 MACF1 DSP NCKAP5 DST BNC2 DENND4C KALRN SSFA2 TMTC2 TIAM1 TNC BMPR1A CALD1 EFNA5 ADGRL2 MYO1E PRICKLE2 PDZRN3 CHD4 GM26917 HNRNPA2B1 COL18A1 EXOC6B MPRIP IFFO2 TRIP12 CSPP1 BAZ2B PHF21A VGLL4 NEDD4 RBMS3 NEAT1 ZAK JAG1 BRWD1 STX7 LAMA3 YME1L1 RAB28 MYO19 KRT5 GJA1 CAR12 EYA3 SAMD5 CREBBP RHOJ MAN1A2 ATP1A1 DDX5 ERBB2IP HIVEP1 CHD9 SYNE2 YWHAQ LDLRAD4 TOX4 D930015E06RIK WAC ANKRD26 MAP3K1 FLNB NFIA ARHGAP24 CPSF6 KHDRBS1 TIAM2 YTHDC1 HR SRRM2 AHNAK KDM2A PFKP LRRC1 SACM1L PDLIM5 MYO1B ABCD3 DDB1 MDM4 ZCCHC14 KTN1 RFWD2 VMP1 RNF41 RTN4 PRR14L

**Pseudo-cell Generation**
**Source:** Provide the first 100 highly expressed genes in an Infundibulum, sorted by expression level:

**Target:** GM42418 CDK8 GPHN IL1RAPL1 JARID2 MALAT1 LARS2 ZC3H7A NEBL NEAT1 NFIA FOS COL1A2 BCL11A NIPBL GPC6 PLXDC2 PARD3 MARCH3 RAB1A TCF12 ZBTB44 EGR1 TMBIM6 SBF2 ARHGAP18 TPM1 EPHB2 LUZP1 SEC31A IDH3A ACTN1 JUN DSP QK METTL5 HEXB MYO1B VCL CHD1 LPCAT3 ID1 SLC20A1 WDR4 IQGAP1 PSD MBD5 FZD6 DDX3Y SNX29 TRIT1 FBXO30 PERP PPL CKAP2 HNRNPDL LCOR LRBA WHSC1 HACE1 HDAC5 KCNIP1 STT3A FUS KATNA1 JUP RFX2 DNM3 P4HB TMEM259 KIF16B MCTP2 PPP2R3C HSPG2 PKN3 TOP2B KIF21A DENND1A IFT43 HJURP RBMS3 GIGYF2 PPP1CB ASXL2 RPS14 MT-CYTB MLLT4 GM15564 COL4A1 DRG1 IKBKB CEP89 PLEC BACH2 RPTOR SMURF2 NUFIP2 ROBO2 FOSL2 TTF2

**Cell Type Annotation**
**Source:** Ascertain the cell type from which these 100 highly expressed genes likely originate. GM42418 IL1RAPL1 GPHN JARID2 CAMK1D CDK8 ZC3H7A LARS2 FGFR2 MALAT1 HEXB RBM25 GPC6 GM26917 YWHAZ EFNA5 FBXW11 NFIB DST ESRP1 RBM26 HADHA PABPC1 CACHD1 BPTF NIN ATP2A2 ERAL1 HACD1 ATF3 CASZ1 ACSL5 CAST SPTLC2 MXD4 IFNGR1 ROBO2 DIMT1 RBMXL1 AMBRA1 SGPL1 SRP68 SGPP1 2510009E07RIK EPCAM MAPRE1 BTBD11 ERBB2IP FBXL17 DYRK1A CD109 TPD52L2 GPR156 EIF3H TCF7L1 SYK CCNK CELF4 ERBB4 HNRNPA0 MRPS16 TNKS2 ZBTB7C TRIP11 TPX2 EEF1D MAT2A PIP4K2B INTS7 PLA2G4F ZCCHC7 FOSB HK2 ZKSCAN17 FAM189A2 NIPBL HMGCS1 SRGAP1 DHX15 LRIG1 RFWD2 JUN INO80D FNIP1 PGLYRP4 LGR4 9330185C12RIK MACF1 SUPT3 CHRNA9 WWC1 SUPT20 BRD4 PNKD RALGPS2 APBB2 NEDD4 RLF SMCHD1 ECT2 Given these genes, the likely corresponding cell type is:
**Target:** TAC-1

**Drug Sensitivity Prediction**
**Source:** Predict the drug sensitivity of a cancer cell to Erlotinib as resistant or sensitive, using its top 100 genes expressed in descending order of expression GSTP1 RPS3 HSP90AA1 PABPC1 GNAS PRDX1 MT-RNR2 RPL18 S100A10 RPL11 RPLP1 RPS6 CCT6A RPS23 GAPDH NQO1 NOP10 FTH1 KRT18 DDX18 KRT13 CCND1 RPL8 HNRNPK MT2A TRMT112 FTL KRT7 TMSB4X LDHB RPS8 SRSF3 PSMA7 RPL27 MGST1 MT-ND4 RPL35A TXN MALAT1 ALDH3A1 BID ARPC2 KRT19 MRPS35 RPL13 PTTG1 HSP90AB1 EPAS1 SERPINB1 SF3B14 NUDT9 EIF3G POLR1D ANAPC11 EIF3D USP22 SKIL CLTA CHCHD4 EIF3H PPP2R5C DHCR7 AC013394.2 ZWILCH RPL4 SOX15 PPP2R1A RPS14 CHCHD6 RPL4P2 RPS12P26 KCTD21-AS1 CHD4 ATP6V1G1 PABPC4 BBX EIF2S1 EI24 MMAB GSTM3 UTP11L RPS15AP38 PREP LTBP3 DHX30 PRDX5 CAPNS1 SERPINB6 ALS2CL POLDIP3 RPS15A GTF2B TOMM7 LSM5 NAPG LSM3 KIF2A NUCKS1 MLLT11 NUDC.
**Target:** sensitive

Figure 9: Examples of single-cell instructions.